Available online at www.sciencedirect.com
SCIENCE DIRECT®
Sensors and Actuators A 116 (2004) 417–423
SENSORS AND ACTUATORS A PHYSICAL
www.elsevier.com/locate/sna

Microsensor for impact of molten metal microdrops

H.-Y. Kim [a,*], T. Karahalios [b], T. Qiu [b], J.-H. Chun [b]

[a] *Thermal/Flow Control Research Center, Korea Institute of Science and Technology, Seoul 136-791, Republic of Korea*
[b] *Department of Mechanical Engineering, Massachusetts Institute of Technology, Cambridge, MA 02139, USA*

Received 23 September 2003; received in revised form 12 May 2004; accepted 25 May 2004
Available online 2 September 2004

Abstract

A microsensor has been developed to measure the spreading of molten metal microdrops upon impact with a solid surface with a time resolution below 1 μs. The sensor consists of fine conducting lines made of a gold (Au) and titanium (Ti) two-layered structure on an insulating surface. The spreading of molten metal on the sensor leads to a resistance drop, which is converted to diameter evolution. Its measurements are made with a digital oscilloscope, which is much faster than state-of-the-art visualization systems. This work demonstrates the ultrafast sensing capability with a molten tin (Sn) microdrop. The sensor is especially useful for measuring the rapid expansion of the contact area in the very early stages of impact, which determines the degree of splashing.

Keywords: Microsensor; Microdrop; Drop impact

1. Introduction

The impact of liquid drops on solid surfaces is fundamental to many industrial processes including erosion [1], spray cooling [2], and fuel–engine wall interaction [3]. To experimentally understand those processes involving water or hydrocarbon drops in general, high-speed photography and videography have been used primarily [4–6]. A drop spreads upon impact with a time scale $\tau = D/U$, with D and U being the drop diameter and the impact velocity, respectively, when impact inertial force dominates capillary and viscous forces [7]. For instance, when a water drop of $D = 3$ mm and $U = 1$ m/s collides with a solid surface, the drop spreads into a thin disk within approximately 3 ms. Considering that high-speed video systems take images at approximately 1000–10,000 frames per second, the "overall" morphology evolution of the foregoing drop can be visualized with conventional techniques.

In addition to the aforementioned applications, the deposition of drops plays a crucial role in such emerging technologies as solder-jet bumping [8] and droplet-based manufacturing [9]. These technologies use "molten metal" drops with diameters ranging from tens to hundreds of micrometers, imposing significant difficulties on optical methods for measuring the drops' dynamic behavior. Molten metal drops are often generated in inert-gas chambers to minimize oxidation, preventing optical access to impinging events. Moreover, the time scale of the microdrop impact process is too small to be resolved by even state-of-the-art, high-speed video systems. For example, the characteristic spreading time of a drop with $D = 300$ μm and $U = 1$ m/s is 300 μs, which may further decrease for a smaller drop and/or a higher impact velocity. As a matter of fact, drop velocity can reach tens of meters per second in spray forming processes, further reducing the characteristic spreading time [10]. Especially, the impact of molten metal drops traveling at high speed often results in splashing, i.e., the unstable expansion of a drop's periphery during spreading, and in extreme conditions even satellite drops are formed. The degree of splashing is determined by an expansion rate in the very early stages of impact [11]. The time range for these steps falls within tens of microseconds and thus is extremely difficult to record with video systems. High-speed photography can, in principle, achieve such a small time resolution, but requires multiple drops having identical impact conditions be reproduced to reconstruct the impact process [5]. Such a task consumes considerable time and is impractical for studying the high-speed impact of molten metal microdrops, for which the drop generation itself is often challenging.

The spreading behavior of molten microdrops challenges current theoretical understanding, as well. Molten drops

* Corresponding author. Tel.: +82-2-958-5673; fax: +82-2-958-6709.
E-mail address: hoyoung@kist.re.kr (H.-Y. Kim).

0924-4247/$ – see front matter © 2004 Elsevier B.V. All rights reserved.
doi:10.1016/j.sna.2004.05.022

spreading on a subcooled solid target undergo a phase change in which thermal parameters, such as temperature, thermal conductivity, specific heat and latent heat, participate in addition to fluid-dynamic parameters as density, surface tension, viscosity, and contact angle. Experimental measurements of such a complex process are essential for clear theoretical understanding. A novel microsensor, therefore, was developed to measure at ultrahigh speed the spreading process of molten metal microdrops. The sensor overcomes the limitations of conventional optical visualization systems in terms of measurement speed and accessibility to the drop deposition area. This paper describes the design and working principle of the spreading sensor. The apparatus and method adopted in this work to deliver a molten metal microdrop to the sensor are also explained. Finally, experimental results that demonstrate the sensor operation are presented.

2. Spreading sensor

Based on the idea that the most significant parameter to be measured during the drop spreading process is the expansion of the drop's base diameter, we designed a microsensor that can generate an electrical signal indicating the diameter of the drop/substrate contact area. A schematic of the microsensor is shown in Fig. 1. The sensor consists of a finely spaced resistance network on an insulating layer. The sensing lines are much finer than shown in the figure, as a sensor surface contains 1250 sensing lines. As a drop spreads on the sensor surface, the closely spaced electrical resistors are covered with molten metal, which is electrically conducting, and consequently are connected electrically. This leads to a drop in the total resistance of the network, R_t, which is given by

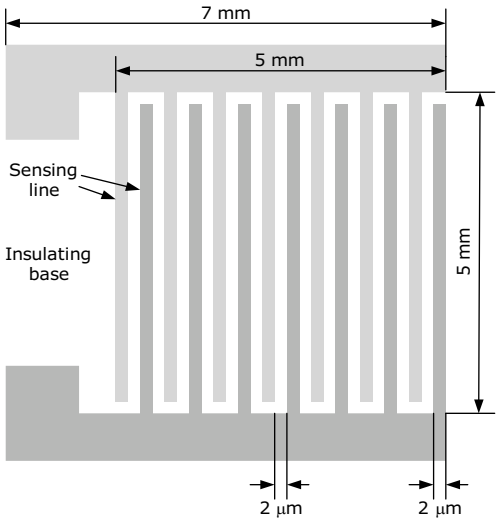

Fig. 1. Schematic of the microsensor.

$$R_t = \left(\frac{1}{R_0} + \frac{N}{R_l}\right)^{-1}, \quad (1)$$

where R_0 is the initial resistance of the sensor, N the number of current paths connected due to the spreading molten metal, and R_l the resistance of the current path. It is assumed that the resistance of each electrical path is the same as the resistance of each sensing line because the microdrop covers only a fraction of the sensor, whose surface measures 5 mm × 5 mm; the dominant resistance to the current thus results from individual sensing lines. The drop base diameter as a function of time, $d(t)$, is related to N as

$$N = \frac{d(t)}{2(\lambda_l + \lambda_s)}, \quad (2)$$

where λ_l and λ_s are the width and the spacing of grid lines, respectively. Combining Eqs. (1) and (2), the evolution of a drop's base diameter can be obtained by measuring the temporal resistance change:

$$d(t) = 2(\lambda_l + \lambda_s) R_l \left(\frac{1}{R_t(t)} - \frac{1}{R_0}\right) \quad (3)$$

Here we note that the microsensor's sensing lines have finite width and spacing, hence the sensor's resistance is converted to a discrete value of the spreading diameter. For illustration, assume that spreading starts from the center of the insulating area between two conducting lines, as shown in Fig. 2. When the contact diameter reaches one spacing, λ_s, two sensing lines are connected and the resistance decreases from its initial value. This resistance remains nearly constant, if the transient period is neglected when the sensing line is incompletely covered, until the spreading metal touches the next sensing lines. Thus the second drop of resistance takes place when the diameter reaches $\lambda_s + 2(\lambda_l + \lambda_s)$. The resistance falls each time the contact diameter increases by $2(\lambda_l + \lambda_s)$ because the number of resistances connected in parallel increases. Therefore, the maximum uncertainty in the diameter corresponding to one resistance value is $2(\lambda_l + \lambda_s)$, which in turn is the measurement resolution.

The width and spacing of the sensing lines should be small enough to spatially resolve the drop spreading process. For the current study, λ_l and λ_s are selected to be 2 μm for a drop size of the order of 100 μm. Gold was used as the sensing line material and silicon oxide as the insulating layer. Titanium was used for the adhesion layer between them. The fabrication process is illustrated in Fig. 3. Fig. 4 shows a scanning electron microscopy (SEM) image of the surface of the microsensor.

The resistance of the individual sensing line is given by

$$R_l = \frac{\rho_e L}{A}, \quad (4)$$

where ρ_e, L, and A are the resistivity, length, and cross-sectional area of the sensing line, respectively. Since thin-film resistivity differs from bulk resistivity, the resistivity of a Ti–Au film deposited on a wafer in the same

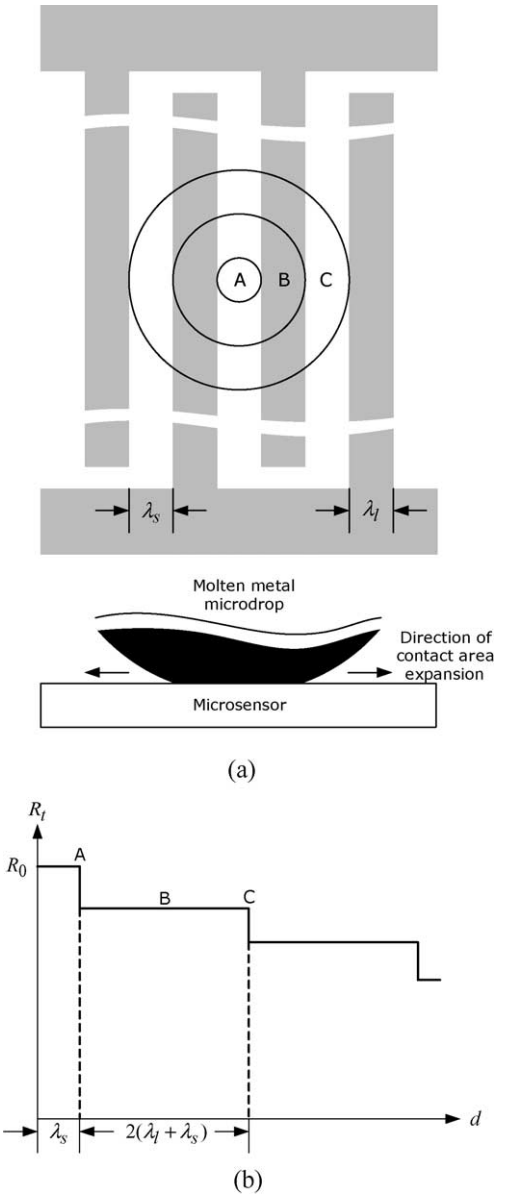

Fig. 2. Relationship between resistance and contact diameter. (a) Increasing spreading diameter upon impact. (b) Resistance change corresponding to increasing diameter.

manner and with the same thickness as the sensing lines of the sensor was measured by the four-point probe method. The film resistivity was measured to be $2.1 \times 10^{-7}\,\Omega$m, thereby giving $R_l = 2.6\,\text{k}\Omega$.

3. Experimental apparatus

To demonstrate the sensor's capability, the following experiment was performed to measure the transient spreading behavior of a molten microdrop. In this work, molten tin (Sn) microdrops were delivered to the sensor by a microdrop generator, shown in Fig. 5. The metal contained in a crucible was melted by a heater and ejected through an orifice with pressure applied from an inert gas supply. The ejected molten Sn formed a laminar jet, which was vibrated by a piezoelectric transducer at a specified frequency. The disturbance due to the vibration grew, due to the Rayleigh instability, until the jet broke up into a stream of uniform drops. This method has an advantage over conventional gas atomization and plasma spray in that the drop size, velocity, and temperature at impact can be obtained precisely while those conventional processes produce molten metal drops in randomly distributed dynamic and thermal states. In addition, the current method generates microdrops with a higher impact velocity than that of molten metal drops generated by a drop-on-demand method [12].

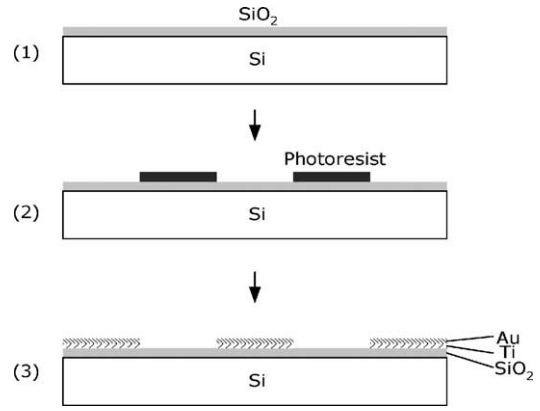

Fig. 3. Microsensor fabrication process: (1) LPCVD (low pressure chemical vapor deposition) of SiO_2. (2) Micropatterning of photoresist. (3) Evaporation of Ti/Au and liftoff to obtain patterned sensing lines.

The initial jet velocity, v_j, and the drop diameter, D, are determined by the nozzle diameter, d_n, the perturbation frequency, f, and the mass flux, $\dot{m}$, using mass conservation:

$$v_j = \frac{4}{\pi}\frac{\dot{m}}{\rho d_n^2}, \tag{5}$$

$$D = \left(\frac{6}{\pi}\frac{\dot{m}}{\rho f}\right)^{1/3}, \tag{6}$$

where ρ is the density of molten Sn. The velocity of a drop, U, and the drop temperature, T, at impact are obtained from the initial velocity, v_j, the initial temperature, and the distance from the generator to the sensor. More details of the computation are presented in [13]. In this work, an orifice 200 μm in diameter, a vibration frequency of 4.22 kHz, and a melt temperature of 300 °C were used. Then the drop impact conditions were such that $D = 373\,\mu$m, $U = 4.15$ m/s, and $T = 281\,^\circ$C (the melting point of Sn is 232 °C). The temperature of the sensor was kept at 27 °C. The Reynolds number and the Weber number, respectively defined as $Re = \rho UD/\mu$ and $We = \rho U^2 D/\sigma$, are non-dimensional parameters determining the fluid dynamic process during spreading. Here μ and σ denote the viscosity and the surface tension, respectively. For this experiment, $Re = 5860$ and $We = 102$, hence the condition falls in an inviscid, impact-driven regime [7].

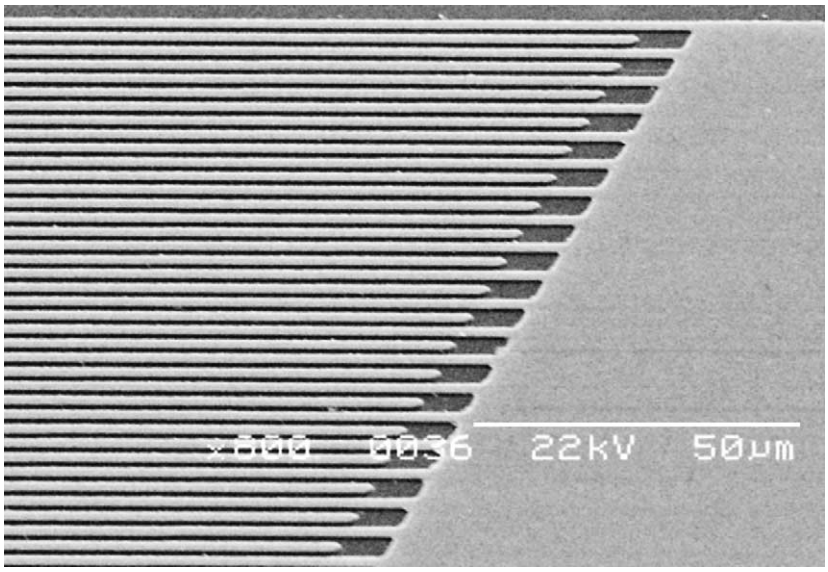

Fig. 4. SEM image of the microsensor surface.

Time evolution of the sensor resistance, R_t, was obtained by measuring the voltage V across the sensor while a constant current I was supplied: $R_t = V/I$. The voltage was recorded by a digital oscilloscope (Tektronix TDS 420A) and a constant current is provided by a DC power supply (HP E3616A). The temporal resolution of the measurement was determined by the data acquisition rate of the oscilloscope, which is much higher than the frame rate of high-speed video techniques. Considering the characteristic spreading time scale of a microdrop used in this study, $\tau = 90\,\mu s$, the sampling rate was set to obtain voltage data every 0.4 μs.

4. Results and discussion

Fig. 6(a) shows the voltage response from the microsensor. The sensor response exhibits initially a rapid voltage drop followed by a mild decrease to about 160 μs. After reaching a minimum, the voltage increases gradually. Since a constant current of 28 mA was supplied, the resistance of the sensor behaved in the same manner as the voltage.

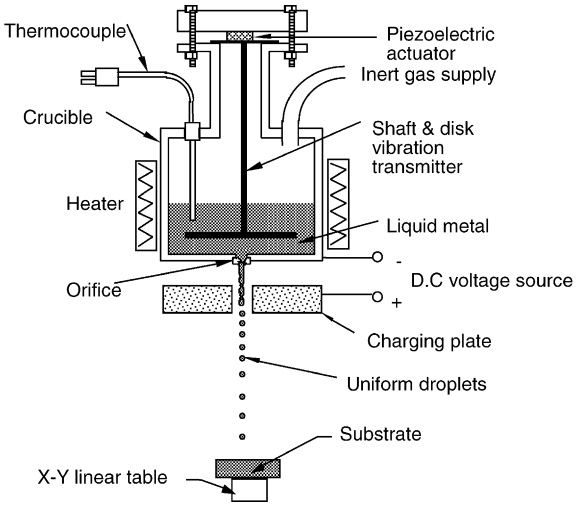

Fig. 5. Schematic of the microdrop generator.

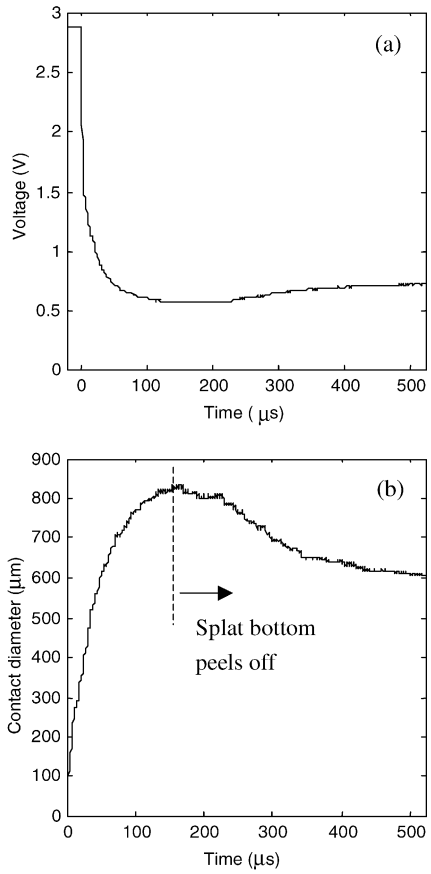

Fig. 6. Measurement results. (a) Voltage response from the microsensor. (b) Diameter evolution as converted from the voltage response.

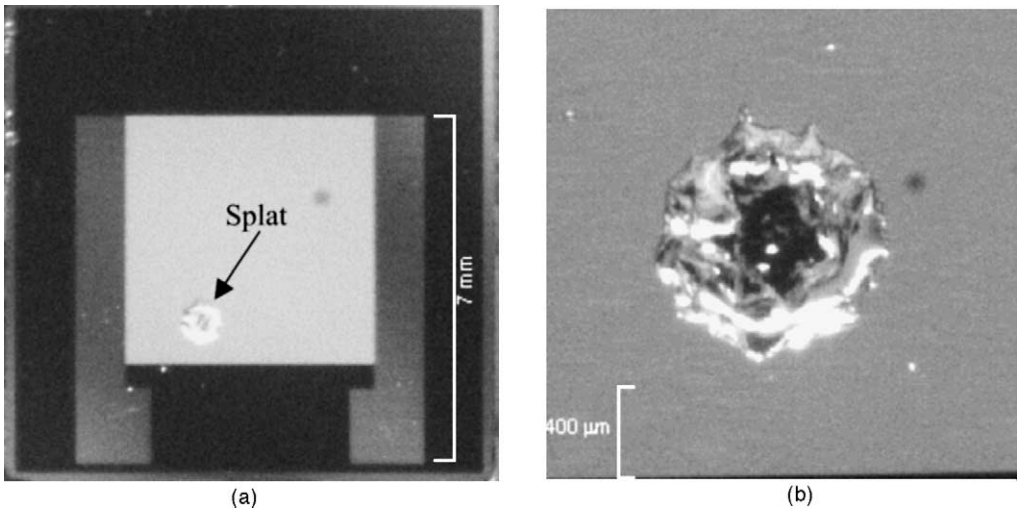

Fig. 7. Micrographs of a pure tin splat deposited on a sensor used for the experiment. (a) Overall view of the sensor and the splat. (b) Magnified top view of the splat.

The signal can be converted to a transient diameter profile by Eq. (3). Fig. 6(b) shows the diameter evolution thus obtained. Upon impact, the drop/substrate contact diameter rapidly increases and the spreading diameter reaches 750 μm in the characteristic spreading time ($\tau = 90\,\mu s$), which amounts to 90% of the maximum spreading diameter (835 μm). The maximum spreading diameter is reached in 166 μs. A micrograph of the splat deposited on the sensor is shown in Fig. 7. Using the image, the splat diameter is measured to be 860 μm, which agrees with the sensor measurement within 3% of error. The fact that the final splat diameter and the maximum spreading diameter measured by the sensor are nearly identical suggests that the increase in sensor resistance after reaching the minimum is not due to the decrease in spreading diameter but to the peel-back of the outer region of the solidifying drop. Therefore, in Fig. 6(b), actual spreading diameter data are confined to the time range from zero to approximately 166 μs. However, the peel-back process recorded by the sensor can be utilized to investigate many important parameters such as the solidification rate and drop/substrate bonding strength.

One of the most prominent advantages of the sensor under investigation is that it can measure spreading area expansion at ultrahigh speed, i.e., as fast as a digital oscilloscope can run. To exploit this merit, the diameter increase in the initial range was investigated. In the very early stage of inertia-driven spreading, which is the case here, it is known that a drop undergoes a kinematic spreading phase in which the rim jet from the bottom of the drop is not yet developed and no morphology change is observable in the descending upper region [14]. After the kinematic phase, a lamella jet emerges from the drop bottom accompanying the collapse of the upper region. Fig. 8(a) compares the experimental data with a theoretical curve representing the kinematic phase [11,14]:

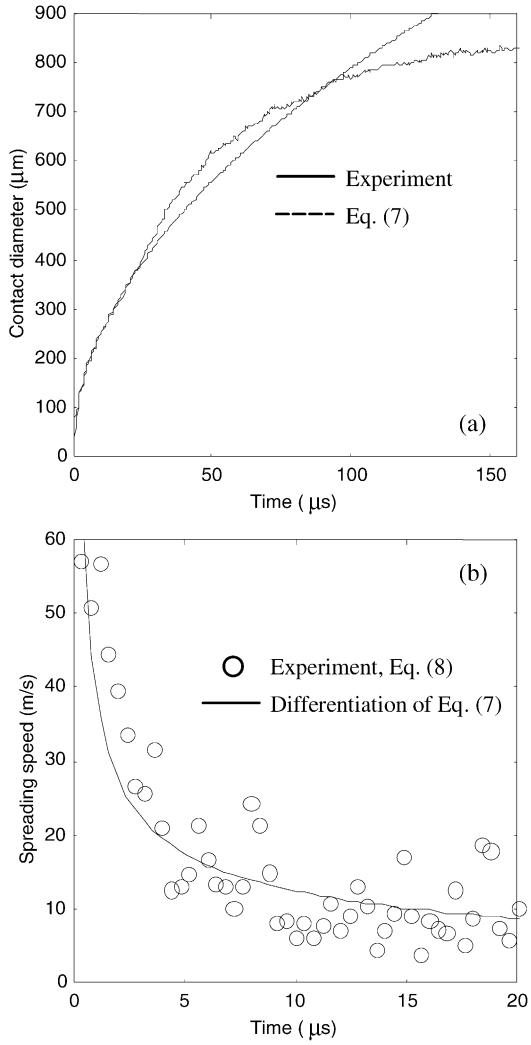

Fig. 8. Initial spreading behavior. (a) Diameter of drop/substrate contact area. (b) Rate of diameter increase.

$$d = 2(DUt)^{1/2}, \tag{7}$$

where d and t denote the drop base diameter and time, respectively. The two curves match until $t = 25\,\mu s$. In experiments with non-solidifying drops, the kinematic phase is reported to last only 0.1τ [14], which corresponds to $9\,\mu s$ in the current drop impact condition. Thus, the lamella jet formation is suppressed longer in the current situation than in ordinary liquid drops, presumably due to solidification at the bottom of the molten drop, which forms a thin solid layer that hampers the lamella ejection.

The experimental data make it possible to calculate the velocity of the drop/substrate contact area expansion in the very early stages of impact. The expansion velocity, v_e, varying with time can be obtained as

$$v_e(t_i) = \frac{d(t_{i+1}) - d(t_i)}{\Delta t}, \tag{8}$$

where Δt is the time difference between the two neighboring measurement moments, t_i and t_{i+1}. Fig. 8(b) shows the expansion speed for the initial 20 μs. The expansion reaches as high as 57 m/s within 1 μs upon impact, about 14 times the original impact velocity. The empirical velocity data are compared with a theoretical curve obtained by differentiating Eq. (7) with respect to time. They show good agreement, reconfirming the initial drop spreading behavior to be a kinematic type.

Despite the sensor's obvious advantage capturing the initial spreading process at ultrahigh speed, limitations exist. Although the initial stages of spreading are independent of a substrate's wetting properties [14], the final stages of spreading when the drop approaches its maximum spreading degree are sensitive to wetting. The selection of sensor materials is limited, thus cannot cover the whole range of wetting conditions. Moreover, the sensor surface exhibits alternating wetting conditions due to insulating and conducting regions. Studying the final stages of spreading on more diverse substrate conditions can be supplemented by conventional optical methods [15], investigation of splat morphology [16], and numerical simulations [9,17]. Still, because the final spreading stages are affected by a drop's spreading history, the microsensor's investigation results for the initial stages are essential to a complete understanding of the process.

5. Conclusions

The spreading sensor developed in this work can measure the contact diameter of a molten metal microdrop and a target surface at ultrahigh speed. Since drop dynamics in the very early stages of impact are independent of substrate wettability, the sensor provides an ideal tool for investigating the rapid expansion of the contact area in that time range. The temporal resolution of the measurement is determined by the sampling rate of a digital oscilloscope, whereas the spatial resolution depends on the pattern dimensions of the sensor. The thinner the sensing lines and their spacing become, the higher the spatial resolution becomes.

An immediate application of this sensor would be to relate the initial rim jet velocity to splashing behavior, as discussed earlier. This relationship is particularly important in the molten metal droplet deposition process, which often suffers from splashing and subsequent satellite drop ejection because metal has a high density and the process involves a high-impact velocity. Such phenomena lead to imperfect drop merging that causes porosity formation, and a poorly controlled drop-solidification rate. That is, satellite drops freeze too fast to merge into a deposition layer that is solidifying. Therefore, a search for optimal deposition conditions for droplet-based deposits and high-quality coatings can be guided by this newly developed microsensor.

References

[1] M.B. Lesser, Analytic solutions of liquid-drop impact problems, Proc. Soc. R. Lond. Ser. A 377 (1981) 289.
[2] M. di Marzo, P. Tartarini, Y. Liao, D. Evans, H. Baum, Evaporative cooling due to a gently deposited droplet, Int. J. Heat Mass Transf. 36 (1993) 4133.
[3] M. Al-Roub, P.V. Farrell, J. Senda, Near wall interaction in spray impingement, SAE Paper No. 960863, 1996, p. 117.
[4] A.M. Worthington, On the forms assumed by drops of liquid falling on a horizontal plate, Proc. Soc. R. Lond. 25 (1877) 26.
[5] S. Chandra, C.T. Avedisian, On the collision of a droplet with a solid surface, Proc. Soc. R. Lond. Ser. A 432 (1991) 13.
[6] H.-Y. Kim, J.-H. Chun, The recoiling of liquid droplets upon collision with solid surfaces, Phys. Fluids 13 (2001) 643.
[7] S. Schiaffino, A. A Sonin, Molten droplet deposition and solidification at low Weber numbers, Phys. Fluids 9 (1997) 3172.
[8] Y.-S. Yang, H.-Y. Kim, J.-H. Chun, Spreading and solidification of a molten microdrop in the solder jet bumping process, IEEE Trans. Comp. Packag. Technol. 26 (2003) 215.
[9] J.-H. Chun, C.H. Passow, Droplet-based manufacturing, CIRP Ann. 42 (1) (1993) 235.
[10] H. Fukanuma, A porosity formation and flattening model of an impinging molten particle in thermal spray coatings, J. Therm. Spray Technol. 3 (1994) 33.
[11] H.-Y. Kim, Z.C. Feng, J.-H. Chun, Instability of a liquid jet emerging from a droplet upon collision with a solid surface, Phys. Fluids 12 (2000) 531.
[12] J.M. Waldvogel, G. Diversiev, D. Poulikakos, C.M. Megaridis, D. Attinger, B. Xiong, D.B. Wallace, Impact and solidification of molten-metal droplets on electronic substrates, J. Heat Transf. 120 (1998) 539.
[13] P. Yim, The role of surface oxidation in the break-up of laminar liquid metal jets, Ph.D. Thesis, Department of Mechanical Engineering, MIT, Cambridge, MA, 1996.
[14] R. Rioboo, M. Marengo, C. Tropea, Time evolution of liquid drop impact onto solid, dry surfaces, Exp. Fluids 33 (2002) 112.
[15] G. Trapaga, E.F. Matthys, J.J. Valencia, J. Szekely, Fluid flow, heat transfer, and solidification of molten metal droplets impinging on substrates: comparison of numerical and experimental results, Metall. Trans. B 23 (1992) 701.
[16] E.W. Collings, A.J. Markworth, J.K. McCoy, J.H. Saunders, Splat-quench solidification of freely falling liquid-metal drops by impact on a planar substrate, J. Mater. Sci. 25 (1990) 3677.

[17] M. Pasadideh-Fard, S. Chandra, J. Mostaghimi, A three-dimensional model of droplet impact and solidification, Int. J. Heat Mass Transf. 45 (2002) 2229.

Biographies

H.-Y. Kim received the B.S. (1994) degree from Seoul National University, Korea, and the S.M. (1996) and Ph.D. (1999) degrees from the Massachusetts Institute of Technology, Cambridge, MA, all in mechanical engineering. He is currently at Thermal/Flow Control Research Center, Korea Institute of Science and Technology in Seoul, Korea. His research interest centers around microfluidics and interfacial flow physics.

T. Karahalios received the B.S. degrees in economics (1998) and mechanical engineering (1999) from the Massachusetts Institute of Technology.

T. Qiu received the B.S. and M.S. degrees from Tsinghua University, China, in 1987 and 1989, respectively, and the Ph.D. degree in mechanical engineering from the University of California, Berkeley, in 1993. He joined the Massachusetts Institute of Technology, Cambridge, as an Assistant Professor in 1994. His research areas include ultrashort light-material interactions, semiconductor processing, heat transfer, and thermal control.

J.-H. Chun received the B.S. degree from Seoul National University, Korea, the M.A.Sc. degree from the University of Ottawa, Canada, and the Ph.D. degree from the Massachusetts Institute of Technology, Cambridge, MA, all in mechanical engineering. At present, he is a Professor of Mechanical Engineering at MIT and Co-Director of the Manufacturing Institute.